Dose distribution effects of spot-scanning proton beam therapy equipped with a multi-leaf collimator for pediatric brain tumors

NOBUYOSHI FUKUMITSU[1], TOMOHIRO YAMASHITA[2], MASAYUKI MIMA[1], YUSUKE DEMIZU[1], TAKESHI SUZUKI[3] and TOSHINORI SOEJIMA[1]

[1]Department of Radiation Oncology, [2]Division of Medical Physics, [3]Department of Anesthesiology, Kobe Proton Center, Kobe, Hyōgo 650-0047, Japan

Received February 25, 2021; Accepted June 15, 2021

DOI: 10.3892/ol.2021.12896

Abstract. The present study simulated the effect of spot-scanning proton beam therapy (PBT) performed using a device equipped with a multi-leaf collimator (MLC) to calculate the dose distribution. Simulation studies using 18 pediatric patients with brain tumors in the posterior fossa were performed. Treatment plans were created for the MLC at different stages: Fully open (initial plan), fully closed to allow an irradiated area extending to 15 mm from the clinical target volume (CTV) (15-mm plan), or closing only the leaves where an organ at risk (OAR) overlapped with a border at 10 or 5 mm from the CTV (10- and 5-mm plans, respectively). The mean dose values for the brainstem, cervical cord, brain and cochlea in all MLC closure plans decreased as the MLC was closed ($P=9.9x10^{-10}$, $P=1.3x10^{-17}$, $P=2.1x10^{-16}$ and $P=2.0x10^{-5}$, respectively). The maximum dose (D_{max}) values of the cervical cord and cochlea in all MLC closure plans were also decreased as the MLC was closed ($P=3.0x10^{-4}$ and $P=1.1x10^{-5}$, respectively). The dose to the CTV was almost unchanged. In 10 patients, the D_{max} of the brain in all MLC-closure plans was higher than that of the initial plan, but the maximum increase was only 0.8 gray relative biological effectiveness [Gy(RBE)]. In conclusion, the existing MLC installed in the treatment device can be used to decrease the OAR dose significantly using spot-scanning PBT without a large capital investment. The dose from the scattered particles was small.

Introduction

Proton beam therapy (PBT) is associated with the emission of high radiation energy after penetration up to a certain depth (1,2) and is widely used for the treatment of various cancer types (3), such as head and neck (4), prostate (5), pediatric brain (6), liver (7) and esophageal (8) cancer. PBT techniques have advanced over the last few decades. One of the most representative advances is the development of the spot-scanning technique using pencil beams (9). Spot-scanning features several dosimetric traits that, depending on the circumstances, can further improve upon conventional passive-scattered broad-beam irradiation; it provides a smaller entrance dose and allows for intensity-modulated treatments that enable dose painting to further spare normal tissue in the vicinity of complex tumor structures. A decrease in the cost of the manufacturing of patient-specific devices, such as compensators, and shorter device adjustment times are other advantages (10-12). The major disadvantage of PBT scanning is the larger lateral penumbra compared with that of passive-scattered beams (13,14). Nevertheless, the number of facilities offering spot-scanning PBT is rapidly increasing worldwide.

Several studies have investigated how to improve the plan quality of spot-scanning PBT using hardware or software systems. Techniques to improve the optimization method and to decrease the size of the penumbra are the main topics of focus. Regarding the development of optimization technology, pencil beam selection (resampling) (15-17) and modified pencil beam positioning, such as contour scanning (18), have been developed. Regarding technology to decrease the penumbra, collimator (19,20) or aperture (21-23) systems have been utilized at some facilities. In addition, a system with four moveable trimmer plates, enabling energy layer-specific collimation [dynamic multi-leaf collimator (MLC)], has been developed (24,25). Furthermore, the combination of using an MLC and contour scanning can reportedly decrease the dose to the organ at risk (OAR) (26).

In contrast to the aforementioned benefits, devices such as collimation systems have the disadvantage of generating scattered particles when interacting with proton beams (27,28). MELTHEA V (Hitachi, Ltd,) is the first commercially available PBT system equipped with a synchrotron that allows switching between a passive-scattered broad-beam and a spot-scanning pencil-beam using the same nozzle. The MLC, which can potentially be used for passive-scattered broad-beam irradiation, can also be used for spot-scanning beam irradiation.

Correspondence to: Dr Nobuyoshi Fukumitsu, Department of Radiation Oncology, Kobe Proton Center, 1-6-8 Minatoshima-Minamimachi, Kobe, Hyōgo 650-0047, Japan
E-mail: fukumitsun@yahoo.co.jp

Key words: spot scanning, proton beam therapy, pediatric brain tumors, multi-leaf collimator

Kobe Proton Center (Kobe, Japan) has a treatment nozzle that can deliver spot-scanning beams and is equipped with an MLC. Dose calculation using the Monte Carlo (MC) method is also available for PBT (29,30). A relatively large number of pediatric patients with cancer are treated at the facility, and necrosis or severe dysfunction of the nervous system are often mentioned as adverse events that should be avoided particularly when treating such patients. The present study investigated the dose distribution benefits and caveats of spot-scanning PBT performed using a device equipped with an MLC by simulating pediatric brain tumors in the posterior fossa.

Materials and methods

Treatment planning system. The treatment planning system consisted of RayStation ver. 9A (Ray Search Laboratories AB), which has a pencil beam dose engine and its own MC dose engine; it transports primary protons and secondary ions (up to α), but does not transport secondary neutral particles, and does not generate δ-ray electrons. MC dose engine starts the transportation upstream of the patient transport grid or the most upstream beam modifier (MLC or range shifter) when used, thus the edge scatter on MLC is included in the calculation. The MC dose engine is described in further detail in the studies by Saini *et al* (29) and Maes *et al* (30). The RayStation uses 1.06 times the projected spot size as the spot distance by default, and this size was not changed for the present study. The optimization algorithm was a sequential quadratic programming method that uses Broyden-Fletcher-Goldfarb-Shanno updates of the quasi-Newton approximation of the Hessian of the Lagrangian (31).

Virtual target study. Three rectangular virtual targets were created with the following dimensions: 4x4x4, 6x6x4 and 8x8x4 cm. The MLC was set at fully open (initial plan) or closed to create irradiation areas with a border at 15, 10 or 5 mm from the target (15, 10- and 5-mm plans, respectively). The beam direction was frontal, and the resulting dose distributions were calculated. Next, the dose distributions were scaled so that the dose received by 50% of the volume (D_{50}) of the targets matched the prescription dose. To assess the benefit of using MLC, lateral penumbras, defined as 80 to 20% of the prescription dose at the target center for each field, were compared for different MLC openings. Also, the maximum dose (D_{max}), which could be increased by scattered particles from the MLC, was compared. In a preliminary study, it was confirmed that spots with an energy deposit located >15 mm away from the target were relatively sparse and had a minimal effect on the dose distribution of the target in this system [number of spots: -5.9%; D_5 of the target: +0.11 Gy(RBE); D_9 of the target: -0.17 Gy(RBE)]. Thus, the present study was started with the MLC closed to create a border at 15 mm from the target.

Analyzing clinical data. Clinical data for a total of 18 pediatric patients with brain tumors in the posterior fossa treated at Kobe Proton Center were studied (age range, 8 months-12 years; mean, 5.8 years; 9 males and 9 females). The primary diseases were medulloblastoma (n=10), ependymoma (n=5) and atypical teratoid/rhabdoid tumor (AT/RT; n=3). The tumors had already been resected, and the post-operative cavities were the targets. The beam directions were left, right and top. Closing the MLC to shield the brainstem impairs the dose of the area on the distant side of the brainstem in the CTV. To minimize the volume of the low-dose area in the CTV, the angle of the top beam was arranged so as to run parallel to the brainstem. The prescription doses [measured in gray relative biological effectiveness: Gy(RBE)] were the same as those used in clinical practice: 27 Gy(RBE) for medulloblastoma, 59.4 Gy(RBE) for ependymoma and 54 Gy(RBE) for AT/RT. For patients with medulloblastoma, brain radiotherapy is usually performed in combination with whole craniospinal irradiation (CSI). Thus, by adding a dose of CSI [23.4 Gy(RBE)] to make a total dose of 50.4 Gy(RBE), the dose difference was decreased among the 3 diseases, making it easier to review and compare.

Table I. Beam parameters.

Beam parameters	Value
Energy, MeV	70.7-235
Energy steps, n	92
Pulse frequency, Hz	1/2.8
Field size, cm	20x15
Source-axis distance (X, Y), m	2.696, 3.029
Scanning speed (X, Y), mm/msec	60, 120
Spot size at isocenter in air, mm (one sigma)	3.3-12
Dose rate, Gy/min	1

Repeated measures single-factor ANOVA was used to compare the dose to the target and organ at risk among the 15-, 10- and 5-mm and initial plans.

Optimization was performed using a pencil beam dose engine. After optimization, the dose distribution was calculated using the MC dose engine for later evaluations. Each beam included a range shifter of 0-6 mm water equivalent thickness made up of polyethylene. Robust optimization with a 4-mm setup and 3.5% range of uncertainty were used. The maximum number of iterations was 40. The main parameters of the beam delivery system are shown in Table I. The clinical goal was to cover the CTV (uniform prescription dose), brainstem [≤52 Gy(RBE) for <8 years; 54 Gy(RBE) for ≥8 years), cervical cord [≤40 Gy(RBE) for <8 years; 43 Gy(RBE) for ≥8 years], brain [≤60 Gy(RBE)] and cochlea [≤43 Gy(RBE)], all converted with an equivalent dose of 2 Gy(RBE).

The first treatment plan was created with the MLC fully open (initial plan). Next, the initial plan was modified by closing the MLC to create an irradiation area with a border at 15 mm from the CTV (15-mm plan); then, only the leaves of the MLC for which the OAR region overlapped with the border at 10 or 5 mm from the CTV were closed (10- and 5-mm plans, respectively). Fig. 1 illustrates these four treatment plans. The dose distribution was calculated for each plan in the same way as that used for the virtual target study.

All the study procedures involving human participants were conducted in accordance with the ethical standards of the institutional research committee (approval no. 30-7), were

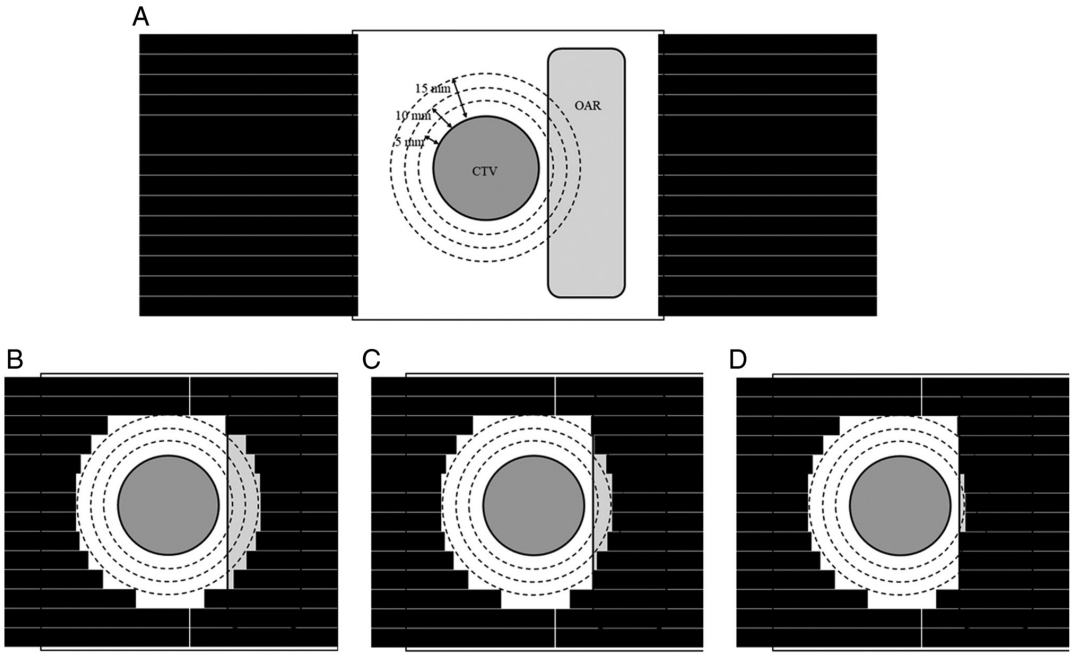

Figure 1. Schema of MLC openings. (A) Initial plan: All leaves of the MLC are fully open. (B) 15-mm plan: All leaves of the MLC are closed to allow a border at 15 mm from the CTV. (C) 10-mm plan: Only the specific leaves of the MLC for which the OAR region overlapped with the border at 10 mm from the CTV are closed. (D) 5-mm plan: Only the specific leaves of the MLC for which the OAR region overlapped with the border at 5 mm from the CTV are closed. MLC, multi-leaf collimator; OAR, organ at risk; CTV, clinical target volume.

in compliance with the Declaration of Helsinki, and were approved by the Institutional Review Board of Kobe Proton Center (Kobe, Japan).

Statistical analysis. Repeated measures single-factor ANOVA followed by Bonferroni's post hoc test, analyzed using Statcel 4 software (OMS Publishing Inc.), was used to compare the dose to the target and OAR among the 15-, 10- and 5-mm and initial plans, and $P<0.05$ was considered to indicate a statistically significant difference.

Results

Virtual target study. The lateral penumbra sharpened as the MLC was closed: From 8.9 to 6.6 mm for a 4x4x4-cm target, from 8.3 to 6.7 mm for a 6x6x4-cm target and from 8.2 to 6.6 mm for an 8x8x4-cm target. For the 10-mm plan, the 95% dose line encompassed the target. For the 5-mm plan, the 95% dose line did not cover the entire target completely. The point of D_{max} was located 1-3 mm upstream of the target close to the beam edge, and the D_{max} tended to increase as the MLC was closed: From 104 to 107% for a 4x4x4-cm target, from 105 to 108% for a 6x6x4-cm target and from 105 to 109% for an 8x8x4-cm target. The dose in the proximal region along the beam edge increased concomitantly as the MLC was closed. All the data are shown in Fig. 2.

Analyzing clinical data. The difference in D_{mean} values of the brainstem, cervical cord, brain and cochlea among the initial, 15-, 10- and 5-mm plan showed significant changes ($P=9.9x10^{-10}$, $1.3x10^{-17}$, $2.1x10^{-16}$ and $2.0x10^{-15}$, respectively). The values showed a decreasing trend as the MLC was closed. The D_{max} of the cervical cord and cochlea also showed significant changes ($P=3.0x10^{-4}$ and $P=1.1x10^{-3}$, respectively). The D_{max} decrease in the cervical cord was 8.3, followed by 5.6 Gy(RBE) in medulloblastoma. Meanwhile, the maximal D_{max} decrease in the cochlea was 8.9, followed by 5 Gy(RBE) in AT/RT and ependymoma. None of the D_{mean}, D_{95} or D_{max} values of the CTV were changed, and only the conformality index of the planning target volume (PTV) (CTV + 5 mm) showed a significant increase ($P=1.7x10^{-3}$). The D_{max} of the skin exhibited no change (Table II and Fig. 3). In 10 patients, the D_{max} of the brain in all MLC-closure plans had a higher value relative to that of the initial plan. The maximum increase was 0.8 Gy(RBE) [from 51.2 to 52 Gy(RBE)] in a patient with medulloblastoma. Fig. 4 shows an example of a patient with AT/RT (8 months old, female). The prescription dose in the initial plan was 27 Gy(RBE) for the post-operative cavity +15 mm and 54 Gy(RBE) for the post-operative cavity +10 mm, but excluding the brainstem. The doses at the brainstem and cochlea were prominently decreased as the MLC was closed, while the dose to the CTV remained almost the same.

Discussion

As the MLC closure increased, from the 15-mm plan to the 5-mm plan, the dose-volume histogram (DVH) curve of the OAR decreased. In particular, when the OAR was shielded to within 10 mm from the CTV (10-mm plan), noticeable decreases were observed in the DVH curves for the brainstem, cervical cord and cochlea. The degree of the volume decrease was more prominent for the low to middle dose level. This can be seen from the fact that the D_{mean} was significantly decreased in most organs in all MLC-closure plans; however, a decrease in D_{max} or D_2 was only observed in the cervical cord and cochlea. This trend is consistent with the study by

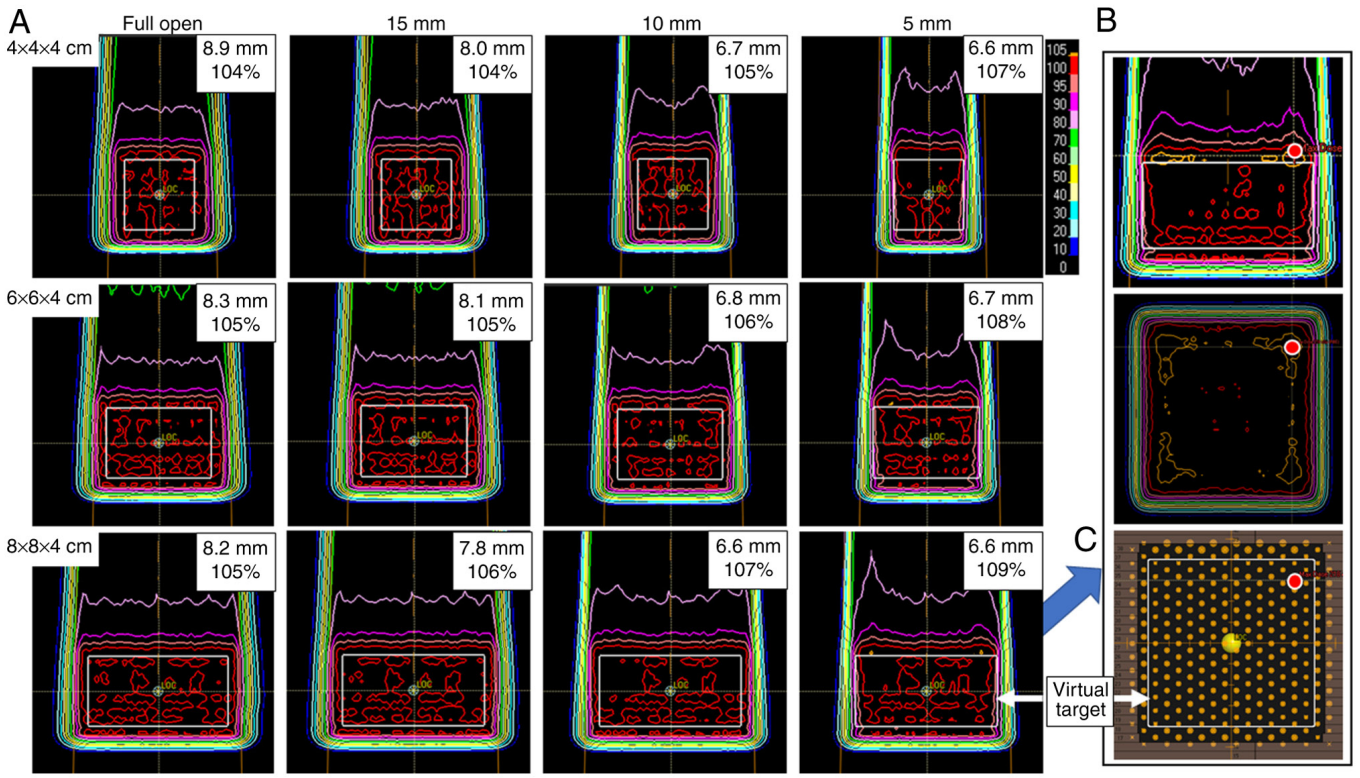

Figure 2. Virtual target study. The target size is 4x4x4 cm (top), 6x6x4 cm (middle) and 8x8x4 cm (bottom). (A) From left to right, the MLC is fully open, and closed 15, 10 and 5 mm to the target. Numbers in the top right of each image are lateral penumbras, defined as 80 to 20% of the prescription dose and maximal doses. (B) The mean vertical and axial images for which the maximal dose site is expressed (target size, 8 cm; MLC margin, 5 mm). (C) The positional relationship between the virtual target, spots and maximal dose site. The red circle indicates the maximal dose site. MLC, multi-leaf collimator.

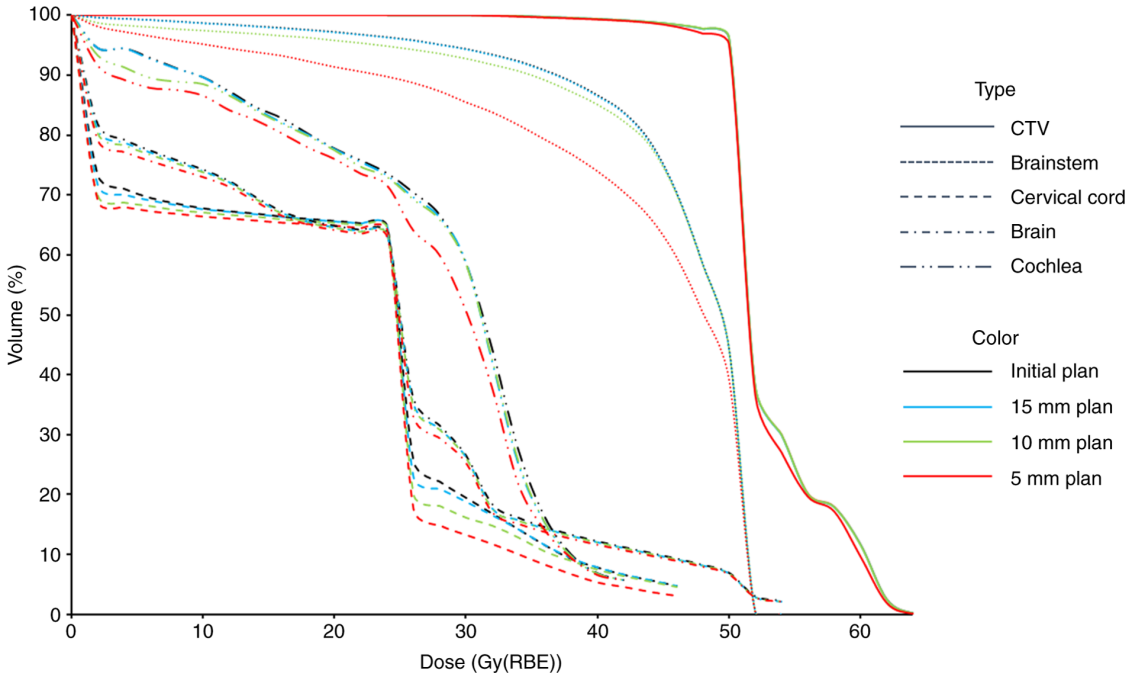

Figure 3. Dose-volume histogram. The type and color of each line are shown in the key. The type classifies the CTV and critical organs, and the color classifies the plan name. CTV, clinical target volume; Gy(RBE), gray relative biological effectiveness.

Sugiyama *et al* (20), in which the use of an MLC decreased the dose mainly in the low-dose area of the lacrimal gland during the treatment of maxillary sinus cancer. Prior to the present study, it was predicted that the D_{max} of the brainstem would also decrease with MLC closure; however, no significant changes in the high-dose parameters were observed in the

Table II. Comparison of dose parameters for each plan.

Parameter	Initial plan	15-mm plan	10-mm plan	5-mm plan	P-value
CTV					
D_{mean}	53.2	53.2	53.2	53.2	0.68
D_{95}	49.4	49.4	49.5	49.5	0.10
D_{max}	55.5	55.5	55.5	55.5	0.09
PTV					
Conformity index	0.4	0.4	0.4	0.39	$1.7x10^{-3a}$
Brainstem					
D_{mean}	46.0	46.0	45.4	42.4	$9.9x10^{-10a}$
D_5	50.3	50.3	50.4	50.3	0.06
D_2	50.7	50.8	50.8	50.8	0.08
D_{max}	51.0	51.0	51.1	51.0	0.11
Cervical cord					
D_{mean}	19.7	19.5	19.0	18.3	$1.3x10^{-17a}$
D_5	38.6	38.6	38.2	34.5	$6.8x10^{-4a}$
D^2	40.8	40.9	40.6	39.0	$9.9x10^{-5a}$
D_{max}	41.7	41.7	41.4	40.0	$3.0x10^{-4a}$
Brain					
D_{mean}	22.2	22.1	22.0	21.6	$2.1x10^{-16a}$
D_5	51.7	51.7	51.6	51.5	0.3
D_2	54.1	54.2	54.1	54.1	0.34
D_{max}	54.6	54.7	54.6	54.6	0.35
Cochlea					
D_{mean}	27.8	27.6	27.2	26.3	$2.0x10^{-5a}$
D_5	32.0	31.9	31.4	30.6	$4.9x10^{-4a}$
D_2	33.2	33.1	32.7	31.7	$1.0x10^{-3a}$
D_{max}	33.7	33.7	33.3	32.3	$1.1x10^{-3a}$
Skin					
D_{max}	25.8	25.7	25.7	25.7	0.41

[a]P<0.05. All data represent gray relative biological effectiveness. D_{mean}, mean dose; D_{max}, maximum dose; D95, dose received by 95% of the volume. CTV, clinical target volume; PTV, planning target volume.

brainstem. We hypothesize that the robustness of the CTV in the treatment planning strongly influenced this result. Since the robustness of the CTV is prioritized in the treatment planning, this method appears to be limited to decreasing the D_{mean} of the brainstem, which is in full contact with the CTV, and this method might not be sufficiently effective to decrease the D_{max}. Regarding the target, the D_{mean} and D_{95} change remained within 1% of the value of the initial plan. Only the conformity index showed a significant difference, but when comparing the individual values, there was no tendency to match the opening and closing of the MLC. Partial permanent hair loss is a serious problem after PBT, especially for female patients. The technique used in the present study is not useful for skin protection as the distance between the skin and CTV is >15 mm in numerous cases. In summary, this OAR shielding technique using an MLC is effective for lowering the OAR dose without affecting the target dose. In particular, in the cervical cord and cochlea, tightening the shielding has the effect of decreasing not only the D_{mean}, but also the D_{max}.

A total of 10 patients were found to have an elevated D_{max} in the brain. This circumstance can also be inferred from the results of the virtual target study. In Fig. 2, an increased dose was observed in the proximal region along the beam edge. In situations where the MLC was closed, the dose at the beam edge increased in a manner that pulled the distribution toward the proximal side, as represented by the bimodal peak of the 80% dose line. As the target size increased, this tendency became stronger, and the two peaks became clearer. This can be interpreted as each peak being generated at the edge of the beam and being released from fusion as the peaks separate from each other. This phenomenon can be considered an effect of the scattering produced by the MLC. Hyer *et al* (32) reported a 2-peak dose profile in a simulation study using the MC method when the collimation system was set to within 1 cm of the target, which is similar to the present data. The clinical impact of an increased dose caused by scattered radiation is important, but the maximum increase was only 0.8 Gy(RBE) in a patient with medulloblastoma. This degree of dose

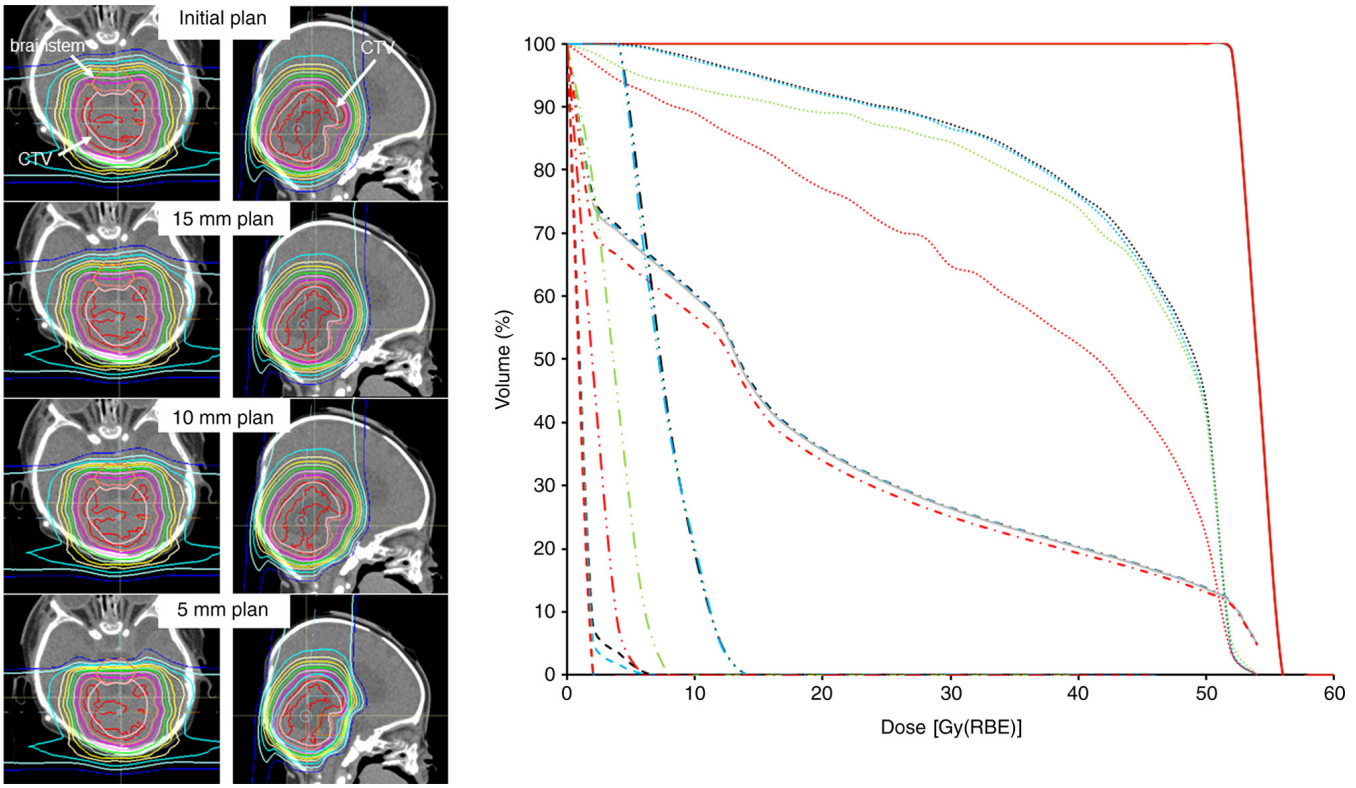

Figure 4. Dose-distribution image and dose-volume histogram of a patient with an atypical teratoid/rhabdoid tumor. CTV, clinical target volume; Gy(RBE), gray relative biological effectiveness.

escalation is usually not clinically important. Therefore, MLC can be considered to have a strong effect, suppressing the dose delivered to the area surrounding the target, such as the OAR, and the dose increase arising from scattered radiation is likely to have little clinical significance.

Several studies attempting to improve the plan quality for spot-scanning PBT using collimation and aperture systems have been performed. Wang *et al* (22) performed a virtual target study and reported that the target dose homogeneity with a 5-mm aperture margin plan was equivalent to the plan without an aperture, but the normal tissue dose was decreased. Dowdell *et al* (21) performed a simulation study using a patient-specific aperture and observed a decrease in the out-of-field dose. Hyer *et al* (10) performed a simulation study using a novel dynamic collimator system. The study reported that it was possible to decrease the OAR dose without changing the target dose, and the dose decrease effect became more marked as the complexity of the target shape increased. In clinical studies, Yasui *et al* (23) reported that a dose decrease in the OAR was obtained in 10 patients with head and neck cancer with no decrease in the CTV dose using an aperture system, and Sugiyama *et al* (20) reported that D_{mean} and D_2 values of the OAR, including the optic nerve and chiasm, were successfully decreased for 26 patients with maxillary cancer using an MLC system. Winterhalter *et al* (26) reported that energy-specific collimation decreased the volume receiving >30% of the prescription dose (V_{30}) outside the PTV by 19.8% in 4 patients with brain and skull base cancer. Regarding pediatric brain tumors, researchers at the University of Iowa and Pennsylvania developed a dynamic collimation and a fixed aperture system, and reported a clear trimming effect, decreasing the OAR dose and increasing the conformity index of the target in 5 patients with brain tumors (24,25). Smith *et al* (24) reported decreases in the D_{mean} of normal tissue adjacent to the target of 13.65 and 5.18% for a dynamic collimation and a fixed aperture system, respectively, and the conformity index improved by 21.35 and 8.38%, respectively. Moignier *et al* (25) reported that the average decrease in the D_{mean} of the brain was 25.1%, and they concluded that a 24.8% decrease in brain necrosis and a 25.1% decrease in the risk of secondary cancer could be expected. Moteabbed *et al* (33) performed a simulation study using a custom-fabricated beam-shaping aperture and range compensator for 14 patients with brain tumor and sarcoma. It was revealed that the device contributed to a decreased OAR dose and that a smaller spot size could further improve the plan quality. Comparing past studies, it is common not only to decrease the dose delivered to the OAR, but also to maintain the dose to the target within the range of a 5- to 10-mm aperture and collimation system. The novelty of the present study is as follows. First, the dose trimming effect and scattered radiation dose derived from the MLC was evaluated while maintaining the target dose for spot-scanning PBT equipped with MLC, which is a relatively new technique, and support for the effect was further verified in a virtual target study. Second, the method can be implemented with existing equipment. This technique does not require a large capital investment, such as a dynamic collimation system, and the irradiation field can be trimmed easily and arbitrarily according to the shape of the lesions and organs, rather than

using a custom-fabricated aperture system. Third, it is noteworthy that the usefulness of the technique was verified in pediatric patients with brain tumors. Based on data reported by Moignier *et al* (25), spot-scanning PBT with MLC can greatly decrease the risk of necrosis or secondary cancer. As pediatric tumors are rare diseases, it is difficult to accumulate and analyze multiple cases. In fact, very few studies applying similar techniques have dealt with pediatric brain tumors. Since Kobe Proton Center is adjacent to one of the largest pediatric hospitals in Japan, it is possible to study numerous cases of pediatric cancer and to obtain data on therapeutic efficacy and safety. We consider it meaningful and novel to examine the dose distribution effect in the largest number of cases so far and to examine the possibility of applying this method to decrease future risks.

As the present study was a simulation study, the various beam parameters were unified. In clinical practice, a total of 12 patients were treated using broad beams before the scanning system was installed, and 3 patients were treated using scanning beams without MLC before the collimation system was equipped with the scanning beam irradiation system; the remaining 3 patients were treated using scanning beams with MLC. In total, 17 of the 18 patients are still alive as of April 2021. The follow-up period was 0.4-2.9 years (median, 1.6 years). Local recurrences occurred in 2 patients. Neurological disorders associated with radiation, such as necrosis, paralysis, audiovisual impairment or abnormal MRI findings, have not been observed.

Although the treatment system used in this study is commercially available, most PBT facilities can use either a scattered broad beam with MLC or a scanning beam without MLC. The development of a collimator system and its external attachment are both expensive and laborious. The development of systems that will allow MLC to be applied to scanning beam irradiation is widely anticipated. The present study investigated the utility of spot scanning using a MLC system for the treatment of brain tumors located in the posterior fossa, assuming the brainstem, cervical cord, brain, cochlea, and skin as OARs. Other organs, such as the optic nerve and the gastrointestinal tract, are also clinically important, and radiotherapy can cause serious adverse events, potentially complicating treatment. Examining the effects at different sites and for different diseases will be a clinically important future prospect.

In conclusion, the present study investigated the effect of spot-scanning PBT combined with MLC using a commercially available system to calculate the dose distribution in pediatric cases with brain tumors located in the posterior fossa. The D_{mean} was decreased in the brainstem, cervical cord, brain and cochlea, and the D_{max} was decreased in the cervical cord and cochlea in the MLC-closure plan, while the dose distribution of the target was maintained. Dose elevation in the brain, probably caused by the scattered beams, was 0.8 Gy(RBE) at most; this value was determined to be small enough not to have a significant clinical impact. Ideally, the leaf margin should be determined by maintaining the target dose, decreasing the OAR dose and minimizing the dose increase to the surrounding organs caused by scattered radiation. The settings differ depending on the system, but in the present system, a setting between 5 and 15 mm was considered ideal.

Acknowledgements

Not applicable.

Funding

This study was supported by Kawano Masanori Memorial Public Interest Incorporated Foundation for Promotion of Pediatrics.

Availability of data and materials

The datasets used and/or analyzed during the current study are available from the corresponding author on reasonable request.

Authors' contributions

NF and TY conceived and designed the study. MM, YD and TSu analyzed the clinical data. NF and TSo analyzed and checked all data and wrote the manuscript. All authors read and approved the final manuscript. NF and TSo confirm the authenticity of all the raw data.

Ethics approval and consent to participate

All the study procedures involving human participants were conducted in accordance with the ethical standards of the institutional research committee (approval no. 30-7), were in compliance with the Declaration of Helsinki and were approved by the Institutional Review Board of Kobe Proton Center (Kobe, Japan). The requirement for informed consent was waived, as the study was a retrospective simulation study.

Patient consent for publication

Not applicable.

Competing interests

The authors declare that they have no competing interests.

References

1. Lawrence JH, Tobias CA, Born JL, Linfoot JA, Kling RP and Gottschalk A: Alpha and proton heavy particles and the bragg peak in therapy. Trans Am Clin Climatol Assoc 75: 111-116, 1964.
2. Bortfeld T and Schlegel W: An analytical approximation of depth-dose distributions for therapeutic proton beams. Phys Med Biol 41: 1331-1339, 1996.
3. Foote RL, Stafford SL, Petersen IA, Pulido JS, Clarke MJ, Schild SE, Garces YI, Olivier KR, Miller RC, Haddock MG, *et al*: The clinical case for proton beam therapy. Radiat Oncol 7: 174, 2012.
4. Holliday EB and Frank SJ: Proton radiation therapy for head and neck cancer: A review of the clinical experience to date. Int J Radiat Oncol Biol Phys 89: 292-302, 2014.
5. Royce TJ and Efstathiou JA: Proton therapy for prostate cancer: A review of the rationale, evidence, and current state. Urol Oncol 37: 628-636, 2019.
6. Haas-Kogan D, Indelicato D, Paganetti H, Esiashvili N, Mahajan A, Yock T, Flampouri S, MacDonald S, Fouladi M, Stephen K, *et al*: National cancer institute workshop on proton therapy for children: Considerations regarding brainstem injury. Int J Radiat Oncol Biol Phys 101: 152-168, 2018.

7. Klein J and Dawson LA: Hepatocellular carcinoma radiation therapy: Review of evidence and future opportunities. Int J Radiat Oncol Biol Phys 87: 22-32, 2013.
8. Chuong MD, Hallemeier CL, Jabbour SK, Yu J, Badiyan S, Merrell KW, Mishra MV, Li H, Verma V and Lin SH: Improving outcomes for esophageal cancer using proton beam therapy. Int J Radiat Oncol Biol Phys 95: 488-497, 2016.
9. Lomax A: Intensity modulation methods for proton radiotherapy. Phys Med Biol 44: 185-205, 1999.
10. Hyer DE, Hill PM, Wang D, Smith BR and Flynn RT: A dynamic collimation system for penumbra reduction in spot-scanning proton therapy: Proof of concept. Med Phys 41: 091701, 2014.
11. DeLaney TF: Proton therapy in the clinic. Front Radiat Ther Oncol 43: 465-485, 2011.
12. Bert C and Durante M: Motion in radiotherapy: Particle therapy. Phys Med Biol 56: R113-R144, 2011.
13. Schippers JM and Lomax AJ: Emerging technologies in proton therapy. Acta Oncol 50: 838-850, 2011.
14. Engelsman M, Schwarz M and Dong L: Physics controversies in proton therapy. Semin Radiat Oncol 23: 88-96, 2013.
15. van de Water S, Kraan AC, Breedveld S, Schillemans W, Teguh DN, Kooy HM, Madden TM, Heijmen BJ and Hoogeman MS: Improved efficiency of multi-criteria IMPT treatment planning using iterative resampling of randomly placed pencil beams. Phys Med Biol 58: 6969-6983, 2013.
16. van de Water S, Safai S, Schippers JM, Weber DC and Lomax AJ: Towards FLASH proton therapy: The impact of treatment planning and machine characteristics on achievable dose rates. Acta Oncol 58: 1463-1469, 2019.
17. Rosas S, Belosi FM, Bizzocchi N, Böhlen T, Zepter S, Morach P, Lomax AJ, Weber DC and Hrbacek J: Benchmarking a commercial proton therapy solution: The Paul Scherrer Institut experience. Br J Radiol 93: 20190920, 2020.
18. Meier G, Leiser D, Besson R, Mayor A, Safai S, Weber DC and Lomax AJ: Contour scanning for penumbra improvement in pencil beam scanned proton therapy. Phys Med Biol 62: 2398-2416, 2017.
19. Bues M, Newhauser WD, Titt U and Smith AR: Therapeutic step and shoot proton beam spot-scanning with a multi-leaf collimator: A Monte Carlo study. Radiat Prot Dosimetry 115: 164-169, 2005.
20. Sugiyama S, Katsui K, Tominaga Y, Waki T, Katayama N, Matsuzaki H, Kariya S, Kuroda M, Nishizaki K and Kanazawa S: Dose distribution of intensity-modulated proton therapy with and without a multi-leaf collimator for the treatment of maxillary sinus cancer: A comparative effectiveness study. Radiat Oncol 14: 209, 2019.
21. Dowdell SJ, Clasie B, Depauw N, Metcalfe P, Rosenfeld AB, Kooy HM, Flanz JB and Paganetti H: Monte Carlo study of the potential reduction in out-of-field dose using a patient-specific aperture in pencil beam scanning proton therapy. Phys Med Biol 57: 2829-2842, 2012.
22. Wang D, Smith BR, Gelover E, Flynn RT and Hyer DE: A method to select aperture margin in collimated spot scanning proton therapy. Phys Med Biol 60: N109-N119, 2015.
23. Yasui K, Toshito T, Omachi C, Hayashi K, Tanaka K, Asai K, Shimomura A, Muramatsu R and Hayashi N: Evaluation of dosimetric advantages of using patient-specific aperture system with intensity-modulated proton therapy for the shallow depth tumor. J Appl Clin Med Phys 19: 132-137, 2018.
24. Smith B, Gelover E, Moignier A, Wang D, Flynn RT, Lin L, Kirk M, Solberg T and Hyer DE: Technical Note: A treatment plan comparison between dynamic collimation and a fixed aperture during spot scanning proton therapy for brain treatment. Med Phys 43: 4693, 2016.
25. Moignier A, Gelover E, Wang D, Smith B, Flynn R, Kirk M, Lin L, Solberg T, Lin A and Hyer D: Theoretical benefits of dynamic collimation in pencil beam scanning proton therapy for brain tumors: Dosimetric and radiobiological metrics. Int J Radiat Oncol Biol Phys 95: 171-180, 2016.
26. Winterhalter C, Meier G, Oxley D, Weber DC, Lomax AJ and Safai S: Contour scanning, multi-leaf collimation and the combination thereof for proton pencil beam scanning. Phys Med Biol 64: 015002, 2018.
27. Smith BR, Hyer DE, Hill PM and Culberson WS: Secondary neutron dose from a dynamic collimation system during intracranial pencil beam scanning proton therapy: A monte carlo investigation. Int J Radiat Oncol Biol Phys 103: 241-250, 2019.
28. Kimstrand P, Traneus E, Ahnesjo A and Tilly N: Parametrization and application of scatter kernels for modelling scanned proton beam collimator scatter dose. Phys Med Biol 53: 3405-3429, 2008.
29. Saini J, Traneus E, Maes D, Regmi R, Bowen SR, Bloch C and Wong T: Advanced Proton Beam Dosimetry Part I: Review and performance evaluation of dose calculation algorithms. Transl Lung Cancer Res 7: 171-179, 2018.
30. Maes D, Saini J, Zeng J, Rengan R, Wong T and Bowen SR: Advanced proton beam dosimetry part II: Monte Carlo vs. Pencil beam-based planning for lung cancer. Transl Lung Cancer Res 7: 114-121, 2018.
31. Gill P, Murray W and Saunders M: Software for large-scale nonlinear programming. User's guide for SNOPT Version 7: 1-116, 2008.
32. Hyer DE, Hill PM, Wang D, Smith BR and Flynn RT: Effects of spot size and spot spacing on lateral penumbra reduction when using a dynamic collimation system for spot scanning proton therapy. Phys Med Biol 59: N187-N196, 2014.
33. Moteabbed M, Yock TI, Depauw N, Madden TM, Kooy HM and Paganetti H: Impact of spot size and beam-shaping devices on the treatment plan quality for pencil beam scanning proton therapy. Int J Radiat Oncol Biol Phys 95: 190-198, 2016.